

# Analysis of a Non-invasive Intracranial Pressure Monitoring Method in Patients with Traumatic Brain Injury



G. Frigieri, R.A.P. Andrade, C. Dias, D.L. Spavieri Jr., R. Brunelli, D.A. Cardim, C.C. Wang, R.M.M. Verzola, and S. Mascarenhas

**Abstract Objective:** We aimed to compare the invasive (iICP) and a non-invasive intracranial pressure (nICP) monitoring methods in patients with traumatic brain injury, based on the similarities of the signals' power spectral densities.

**Materials and methods:** We recorded the intracranial pressure of seven patients with traumatic brain injury admitted to Hospital São João, Portugal, using two different methods: a standard intraparenchymal (iICP) and a new nICP method based on mechanical extensometers. The similarity between the two monitoring signals was inferred from the Euclidean distance between the non-linear projection in a lower dimensional space (ISOMAP) of the windowed power spectral densities of the respective signals. About 337 h of acquisitions were used out of a total of 608 h. The only data exclusion criterion was the absence of any of the signals of interest.

**Results:** The averaged distance between iICP and nICP, and between arterial blood pressure (ABP) and nICP projections in the embedded space are statistically different for all seven patients analysed (Mann-Whitney  $U$ ,  $p < 0.05$ ).

**Conclusions:** The similarity between the iICP and nICP monitoring methods was higher than the similarity between

the nICP and the recordings of the radial ABP for all seven patients. Despite the possible differences between the shape of the ABP waveform at radial and parietal arteries, the results indicate—based on the similarities of iICP and nICP as functions of time—that the nICP method can be applied as an alternative method for ICP monitoring.

**Keywords** Non-invasive · Intracranial pressure · Arterial blood pressure · Dimensionality reduction · Fourier transform

## Introduction

Intracranial pressure (ICP) is usually monitored via the insertion of a catheter and pressure transducer into the subdural, epidural, subarachnoid, intraventricular or intraparenchymal spaces [1]. Potential disadvantages of these methods are the risk of bleeding and infection, calibration problems and obstructions, operation restricted to a neurosurgical environment and high associated cost. In view of these downsides, there have been several initiatives to develop non-invasive methods to continuously monitor ICP [2–5]. We present here the application of a new non-invasive ICP (nICP) monitoring method based on mechanical extensometers.

The new non-invasive monitoring method consists of a strain gauge (mechanical extensometer) fixed on a mechanical device that touches the scalp in the parietal region lateral to the sagittal suture. The non-invasive sensor is able to detect small skull deformations resulting from changes in ICP. In the current state of development, this method does not yet yield pressure values calibrated in millimetres of mercury, but can deliver continuous information about the ICP waveform.

The ICP waveform is directly related to cerebral compliance. The cardiac component of ICP typically comprises three peaks: P1, associated with the systolic blood pressure

---

G. Frigieri (✉) · R.A.P. Andrade · D.L. Spavieri Jr. · C.C. Wang  
Braincare, São Carlos, SP, Brazil  
e-mail: [g.frigieri@gmail.com](mailto:g.frigieri@gmail.com)

C. Dias  
Hospital São João, Universidade do Porto, Porto, Portugal

R. Brunelli · S. Mascarenhas  
Braincare, São Carlos, SP, Brazil

Instituto de Física de São Carlos, Universidade de São Paulo,  
São Carlos, SP, Brazil

D.A. Cardim  
Brain Physics Laboratory, Division of Neurosurgery, Department  
of Clinical Neurosciences, University of Cambridge,  
Cambridge, UK

R.M.M. Verzola  
Department of Biological Sciences and Health, Federal University  
of São Carlos, São Carlos, SP, Brazil

wave transferred by the choroid plexus to the cerebrospinal fluid; P2, associated with the reflection of systolic wave into the parenchymal tissue; P3, related to the closure of the aortic valve. By observing only the relative amplitude of peaks P1, P2 and P3, it is possible to obtain relevant clinical information. For example, an increase of the amplitude of the three peaks indicates an increase of the mean ICP. A reduction in the P1 amplitude suggests loss of cerebral perfusion, and an increase in P2, loss of brain compliance. Fusion of the peaks P1, P2 and P3 associated with a high mean amplitude may indicate that the autoregulation of the cerebrovascular system is not properly functioning [6–10].

In this study, we compare the waveforms of standard invasive ICP (iICP) and nICP in a lower dimensional space constructed based on signals in the frequency domain. Our goal was to verify the similarities between the two ICP waveforms—invasive and non-invasive—and the radial arterial blood pressure (ABP) along all recording time, without having to look at high dimensional signals directly. In a lower dimensional space, we can see when and how the non-invasive method waveform follows the invasive method as a function of time as changes in ICP occurred.

The comparison between invasive and non-invasive ICP waveforms aim to validate the non-invasive method as an alternative to invasive measurements in situations where the waveform can give additional clinical information. We also compared the nICP with arterial ABP waveforms to verify the possible influence of the peripheral circulation into the nICP signal, which is one of the possible limitations of the present method.

## Materials and Methods

The non-invasive sensor consists of a support for a sensor bar for the detection of local skull bone deformations, adapted with extensometers. Detection of these deformations is obtained by a cantilever bar modelled by finite elements calculations. To this bar, strain gauges are attached for strain detection. Non-invasive contact with the skull is obtained by adequate pressure directly on the scalp by a pin. Changes in ICP cause deformations in the skull bone detected by the sensor bar. Variations in ICP lead to deformations in the bar, which are captured by the strain sensors. The equipment filters, amplifies and digitalises the signal from the sensor, and sends the data to a computer [11].

We recorded the ICP of seven patients with traumatic brain injury admitted to Hospital São João, Portugal, using two different methods: a standard intraparenchymal micro-transducer (Codman & Shurtleff, Raynham, MA, USA) and

the non-invasive method (Braincare, São Paulo, Brazil), placed on the parietal region of the patient’s scalp using an elastic head band. We also recorded the ABP through the radial artery and the partial pressure of carbon dioxide (PaCO<sub>2</sub>) simultaneously. We analysed approximately 337 h of recordings from a total of 608 h. The only exclusion criterion was the absence of any of the signals of interest. Table 1 presents the patients’ demographics and average recording time for each individual.

The similarity between two time-series at a given temporal window was inferred from the Euclidean distance between the non-linear projection in a lower dimensional space of the windowed power spectral densities of the respective signals. We calculated the power spectral density of the signal  $x$  using the short-time Fourier transform [12]:

$$\text{STFT}[x(n)]_m = \sum_{n=-\infty}^{\infty} x[n]w[n-m]e^{-j\omega n}$$

where  $w[k]$  is the Blackman window. We used window length of 10 s, with a sampling frequency of 250 Hz. We then reduced the dimensionality of STFT (250 dimensions) space to two dimensions using a non-linear dimensionality reduction algorithm (ISOMAP) [13], in which the embedding is done in three steps. First, we calculated the Euclidean distances between the power spectral densities (PSD) of the windowed signals. In the second step, we constructed a graph based on the nearest neighbours of the PSDs; in the final step, we performed classical multidimensional scaling using the geodesical distances between nodes on the graph to embed the signal into the lower space. A schematic representation of the data processing pipeline can be seen in Fig. 1. The whole analysis was performed using custom programs written in the python language, using the libraries Scipy [14], Matplotlib [15] and Scikit-learn [16].

**Table 1** Overview of the data analysed

Patient	Age	Gender	Pathology	Acquisition time (h)
1	52	F	Spontaneous haemorrhage	282
2	70	M	Brain tumour	97.8
3	65	M	Brain tumour	77.1
4	77	M	Traumatic injury	37.6
5	72	F	Spontaneous haemorrhage	141.1
6	33	F	Spontaneous haemorrhage	68.3
7	56	F	Traumatic injury	141.1

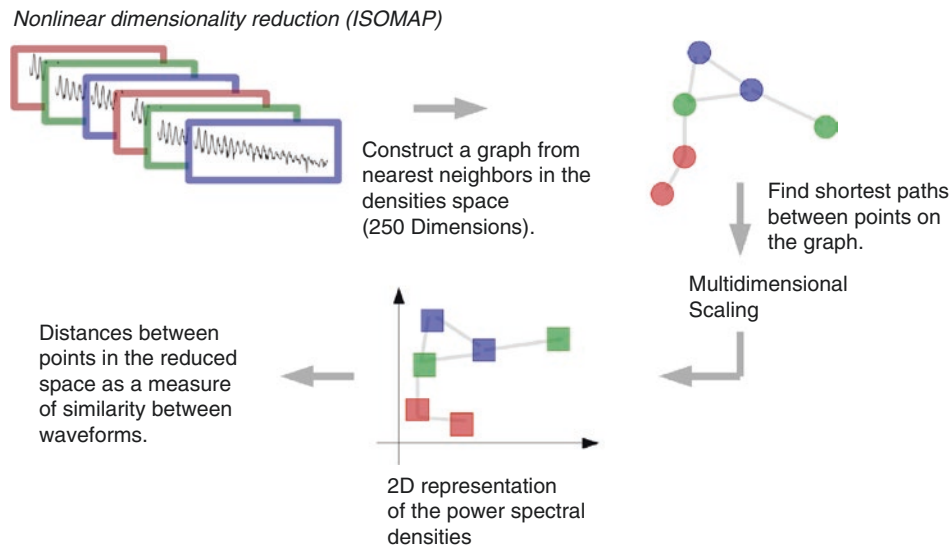


**Fig. 1** Schematic representation of the data processing pipeline

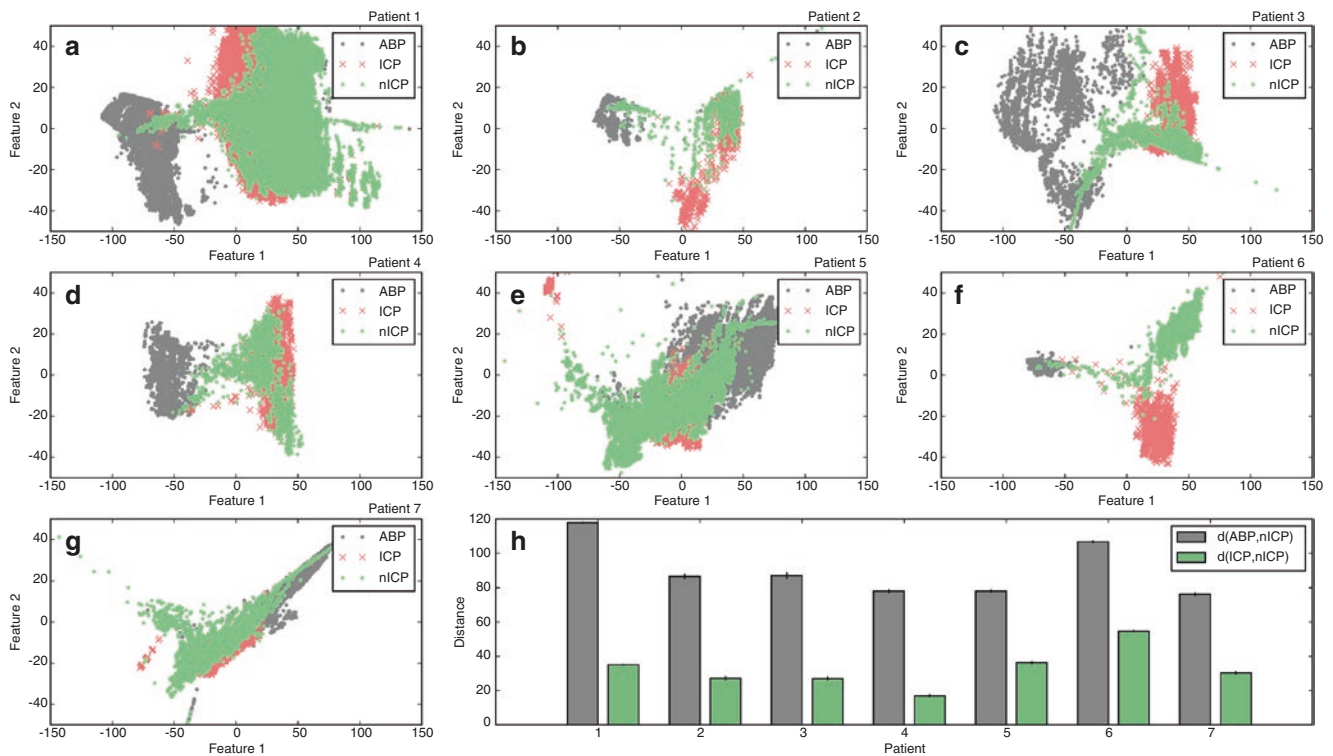


**Fig. 2** Projection of the power spectral density into a lower dimensional space for seven patients with traumatic brain injury (a–g). (h) Average distances for iICP-nICP and ABP-nICP projections for the

seven patients. Errors bars are non-parametric confidence intervals with  $\alpha = 0.05$  and 1000 replications

**Results**

The ISOMAP projection of the PSD signals of six patients can be observed in the Fig. 2. Each point on the graphs in Fig. 2a–g represents the PSD of a 10-s window of the respective signals embedded into the lower dimensional space. We can qualitatively observe that nICP and iICP points are on

average closer than ABP and iICP points for most of the patients. Indeed, the average distances between the respective points confirm that (Fig. 2h, Table 2). The differences between iICP-nICP and ABP-nICP are statistically significant for all seven patients (Mann-Whitney  $U$ ,  $p < 0.05$ ). A dynamic comparison as a function of time can be seen at the following link (<https://youtu.be/dK1XK-4jCkE>). The

**Table 2** Measure of similarities between iICP, ABP and nICP for seven patients (arbitrary units)

Similarities	Patient ID						
	1	2	3	4	5	6	7
iICP-nICP	35.0	27.2	26.9	16.9	36.3	54.7	30.3
ABP-nICP	117.3	86.6	86.9	77.9	78.1	106.6	76.3

video shows the representation of three signals—iICP (red), nICP (green) and ABP (grey)—for one patient during 24 h. In the upper panel, one can observe the nonlinear projection of the three signals power spectral densities, which are shown in the lower right panel. In the lower left panel, one can see the corresponding morphologies.

## Discussion

We did not expect that the waveforms—and respective frequency domain signatures—of the ICP recording methods were identical, because they are recorded at different sites—one inside the parenchyma and other outside the skull. Both waveforms are, however, an indirect result of mechanical waves generated by the blood inflow to the brain and, therefore, should share some similarities. Indeed, we were able to observe a dynamic similarity between the waveforms as ICP changed in time. Given the importance of ICP waveform analysis to monitor the clinical state of the patient, and the similarities between the invasive and non-invasive methods, we suggest that the non-invasive method can be used for monitoring relative changes in ICP despite the absence of absolute values in mmHg.

One possible limitation of the non-invasive method could be the interference of peripheral circulation on the nICP signal. We therefore compared the iICP and nICP waveforms with the radial artery blood pressure waveform, and observed that similarities between nICP and iICP are greater than the similarities between ABP and nICP or ABP and iICP. Nevertheless, such limitation could be minimised if the non-invasive sensor positioning is optimised, i.e. away from major vessels in the parietal region. This could attenuate the potential influence of the peripheral circulation on the nICP waveform, and consequently approximate its pattern to the direct ICP waveform.

## Conclusions

The waveform similarity between iICP and nICP methods was greater than the similarity between nICP and radial ABP for all seven patients. Despite the possible differences between the shape of the ABP waveform at radial and parietal arteries, the results indicate—based on the similarities of iICP and nICP as functions of time—that the nICP method can be used as an alternative tool for ICP monitoring in

conditions where the knowledge of absolute values might not be essentially relevant.

**Acknowledgements** Funded by FAPESP, PAHO, CNPq and Ministry of Health of Brazil.

**Conflicts of interest statement** We declare that we have no conflict of interest.

## References

1. Lee KR, Hoff JT. Intracranial pressure. In: Youmans JR, editor. *Youmans neurological surgery*, vol. 1. 4th ed. Philadelphia: WB Saunders; 1996. p. 491–518.
2. Kashif FM, Verghese GC, Novak V, Czosnyka M, Heldt T. Model-based noninvasive estimation of intracranial pressure from cerebral blood flow velocity and arterial pressure. *Sci Transl Med*. 2012;4:129ra44.
3. Ragauskas A, Daubaris G, Dziugys a, Azelis V, Gedrimas V. Innovative non-invasive method for absolute intracranial pressure measurement without calibration. *Acta Neurochir Suppl*. 2005;95:357–61.
4. Barone DG, Czosnyka M. Brain monitoring: do we need a hole? An update on invasive and noninvasive brain monitoring modalities. *Sci World J*. 2014;2014:1–6.
5. Padayachy LC. Non-invasive intracranial pressure assessment. *Childs Nerv Syst*. 2016;32:1–11.
6. CJJ A, Van Eijndhoven JH, Wyper DJ. Cerebrospinal fluid pulse pressure and intracranial volume-pressure relationships. *J Neurol Neurosurg Psychiatry*. 1979;42:687–700.
7. Hashimoto M, Higashi S, Tokuda K, Yamamoto Y, Yamashita J. Changes of intracranial pressure and pulse wave form induced by various mechanical stresses upon intracranial hemodynamics. In: Avezaat CJJ, van Eijndhoven JHM, Maas AIR, Tans JJJ, editors. *Intracranial pressure*. VIII SE—79. Heidelberg: Springer; 1993. p. 367–71.
8. Ferreira MCPD. Multimodal brain monitoring and evaluation of cerebrovascular reactivity after severe head injury. Porto: University of Porto; 2015.
9. Fan JY, Kirkness C, Vicini P, Burr R, Mitchell P. Intracranial pressure waveform morphology and intracranial adaptive capacity. *Am J Crit Care*. 2008;17:545–54.
10. Scalzo F, Hamilton R, Hu X. Real-time analysis of intracranial pressure waveform morphology. In: Chen K-S, editor. *Adv Top Neurol Disord InTech*. 2012;99–128.
11. Cabella B, Vilela GHF, Mascarenhas S, Czosnyka M, Smielewski P, Dias C, Colli BO (2016) Validation of a new noninvasive intracranial pressure monitoring method by direct comparison with an invasive technique. *Acta Neurochirurgica. Supplement* 2016;122:93–96.
12. Allen J. Short term spectral analysis, synthesis, and modification by discrete Fourier transform. *IEEE Trans Acoust Speech Signal Process*. 1977;25(3):235–8.
13. Tenenbaum JB, de Silva V, Langford JC. A global geometric framework for nonlinear dimensionality reduction. *Science (New York, N.Y.)*. 290(5500), 2319–23.
14. Jones E, Oliphant T, Peterson P. *Scipy: open source scientific tools for Python*. 2001. <http://www.scipy.org>.
15. Hunter JD. Matplotlib: a 2D graphics environment. *IEEE Comput Sci Eng*. 2007;9:90–5.
16. Pedregosa F, Varoquaux G, Gramfort A, Michel V, Thirion B, Grisel O, et al. Scikit-learn: machine learning in Python. *J Mach Learn Res*. 2011;12:2825–30.